The g_J Factor of an Electron Bound in Hydrogen-Like Carbon: Status of the Theoretical Predictions

Thomas Beier[1,2], Ingvar Lindgren[2], Hans Persson[2], Sten O. Salomonson[2], and Per Sunnergren[2]

[1] GSI, Atomphysik, Planckstr. 1, DE-64291 Darmstadt, Germany
[2] Department of Physics, Chalmers University of Technology and Göteborg University, S-412 96 Göteborg, Sweden

Abstract. We present the known theoretical contributions to the g_J factor of an electron bound in hydrogenlike carbon. In particular we outline the calculation scheme for the quantum electrodynamical (QED) corrections of order (α/π) and present their current theoretical uncertainties. The known terms of the $(Z\alpha)$ expansion are found to be insufficient to describe the current experimental data.

1 Introduction

Highly charged ions provide a unique testing ground for quantum electrodynamics (QED) in very strong electric and magnetic fields which otherwise are not experimentally accessible [1]. Very precise measurements have been performed on the Lamb shift in hydrogenlike [2,3] and lithiumlike [4,5,6] heavy systems and also on the hyperfine structure (HFS) splitting [6,7,8,9]. Another quantity suitable for investigating QED of strong fields is the Zeeman level splitting of a hydrogenlike atom under the influence of an external magnetic field. The energy shift due to this external field is given by

$$E_{\mathrm{mag}} = \langle\, -\boldsymbol{\mu}\cdot\boldsymbol{B}\,\rangle \tag{1}$$

where the magnetic moment $\boldsymbol{\mu}$ of a rotating charge q with mass m_q is related to its angular momentum $\boldsymbol{J}$ by the g factor,

$$\boldsymbol{\mu} = g_J\,\frac{q}{2\,m_q\,c}\,\boldsymbol{J}\ . \tag{2}$$

For an electron, $q=-e$, and

$$\boldsymbol{\mu} = -g_J\,\frac{e}{2\,m_e\,c}\boldsymbol{J} = -g_J\,\mu_B\,\frac{\boldsymbol{J}}{\hbar}\ , \tag{3}$$

where μ_B is the Bohr magneton. For a free electron the g_S factor of its spin was measured by Van Dyck *et al.* [10] who obtained $g_S = 2+2\times 1\,159\,652\,188.4(4.3)\times 10^{-12}$. The deviation from the Dirac value of 2 is due to QED effects and the

value obtained from the calculations (for a recent overview cf. [11]) is in complete agreement. The measurement is thus one of the most stringent tests of QED of a free particle.

Contrary to this outstanding success, investigations on the bound-state QED modifications to g_J were rather sparse until the mid 1990's. Grotch and Hegstrom [12,13,14] as well as Faustov [15,16] and Close and Osborn [17] performed calculations on the first terms of a $(Z\alpha)$ expansion for QED and recoil corrections to g_J. Experiments were carried out on hydrogen and deuterium ([18,19,20] and references therein) as well as on He^+ [21]. The existing theoretical calculations were then sufficient to describe the experimental results.

Recently, a new setup was developed [22] and tested [23] which allows the storage of a single hydrogenlike ion in a trap and the performance of g_J measurements with a precision up to a few ppb [24]. Up to now, experiments have been carried out on $^{12}C^{5+}$ but are planned to be extended to systems up to U^{91+}. The most recent experimental value is presented in detail elsewhere in this volume [25]. The experimental success demands a close look on the theoretical contributions to the g factor of an electron bound in a hydrogenlike system. In the following we will present the current status of these effects for the case of carbon.

2 Pure Binding and Nuclear Effects

For a bound electron, the spin is no observable quantity. Only the total angular momentum $\boldsymbol{J}$ can be observed. The energy shift of a state $|a_n\rangle$ due to an external magnetic field (for simplicity assumed to point along the z-direction) is given by

$$\Delta E = -\langle a_n|\boldsymbol{\mu}\cdot\boldsymbol{B}|a_n\rangle = g_J\frac{\mu_B}{\hbar}B_z\langle a_n|J_z|a_n\rangle = \frac{1}{2}g_J\mu_B B_z \tag{4}$$

for an electron with $|a_n\rangle = |1S_{1/2}\rangle$ and magnetic angular quantum number $m = 1/2$. This can be also written as

$$\Delta E = \langle a_n|\boldsymbol{\alpha}\cdot e\mathbf{A}|a_n\rangle \tag{5}$$

where

$$\boldsymbol{A} = -(\boldsymbol{r}\times\boldsymbol{B})/2 \tag{6}$$

which leads to

$$g_J = 2\left[\frac{1+2\sqrt{1-(Z\alpha)^2}}{3}\right], \tag{7}$$

for an electron bound to a point-like nucleus. Only in this case is the analytical calculation of all appearing integrals possible. The result is due to Breit [26]. For $^{12}C^{5+}$ this yields a value of $g_{J,\,\mathrm{Breit}} = 1.998\,721\,354\,2$.

The finite size of the nucleus leads to slighlty altered wave functions in (4) and (5) and thus to a deviation from the value given by (7). This deviation amounts

to the order of 10^{-3} for heavy systems like uranium but is only 4×10^{-10} for carbon and thus even below the current experimental precision.

Another contribution due to nuclear properties is the so-called recoil contribution. It takes into account the finite mass of the nucleus even beyond the non-relativistic reduced mass approximation. Up to now there is a lack of calculations non-perturbatively in $(Z\alpha)$ which exist only for the QED corrections of order (α/π) up to now but would definitely be required for heavy systems.

Expressions for the leading terms of an expansion in (α/π), $(Z\alpha)$, and the mass-ratio electron/nucleus, (m_e/M_N) were obtained in 1970 independently by Grotch [13,14] utilizing an expansion of the corresponding two-particle Dirac equation, and also by Faustov [16], who employed an effective potential method. Their results were reproduced by Close and Osborn [17] starting from a group theoretical approach. The recoil contribution known so far reads

$$g_{J,\,\mathrm{recoil}} = (Z\alpha)^2 \left[\left(\frac{m_e}{M_N}\right) - (1+Z)\left(\frac{m_e}{M_N}\right)^2 \right] + (Z\alpha)^2 \left(\frac{\alpha}{\pi}\right) \left[-\frac{1}{3}\left(\frac{m_e}{M_N}\right) + \frac{3-2Z}{6}\left(\frac{m_e}{M_N}\right)^2 \right] \tag{8}$$

which is exact to orders $(Z\alpha)^2$, (α/π), and $(m_e/M_N)^2$. For hydrogenlike carbon, this yields a recoil correction of 8.75×10^{-8} to g_J where a relative uncertainty of 1 % should be assumed because of considering only the leading terms in a $(Z\alpha)$ expansion. We stress that this uncertainty increases for heavier systems and might amount to about 10 % for Ca already [27].

The internal structure of the nucleus might also affect the g_J factor. The nucleus can be envisaged as consisting of protons and neutrons which in turn are formed by quarks and gluons. This composite object can undergo a virtual excitation and deexictation exchanging two photons with the propagating electron, called nuclear polarization. In electronic systems, evaluations of the nuclear polarization effect have been carried out only as corrections to the QED Lamb shift predictions for the lowest-lying states of heavy few-electron ions (cf. [1] and references therein) and not yet for the g_J factor. However, it is thought to be completely negligible for light systems as C^{5+}.

3 QED Effects of Order (α/π)

The QED contributions of order (α/π) (i.e., one internal photon line in the corresponding Feynman diagram) form the major QED contribution to the g factor. For g_S they comprise only one diagram which was evaluated already in 1947 by Schwinger [28,29]. If the electron is bound, the number of diagrams which have to be considered, increases. All diagrams are depicted in Fig. 1. The leading term of a $(Z\alpha)$ expansion was given by Grotch [12]. Results from a non-perturbative calculation were presented by Blundell *et al.* for the self-energy part of the diagrams [30] and by Persson *et al.* for all diagrams [31,32].

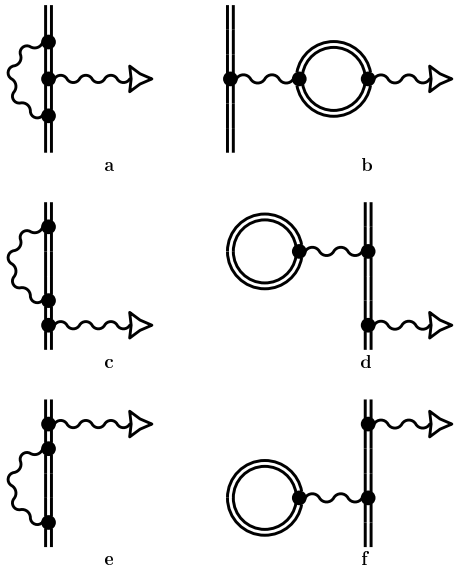

Fig. 1. The QED contributions of order (α/π) to the bound-electron g_J factor depicted as Feynman diagrams. Double lines indicate bound fermions, wavy lines indicate photons. The interaction with the magnetic field is denoted by a triangle. Diagram (a) is also termed "SE, ve" (self-energy vertex correction), diagrams (c) and (e) "SE, wf" (self-energy wave-function correction), diagram (b) "VP, pot" (vacuum-polarization potential correction), and diagrams (d) and (f) "VP, wf" (vacuum-polarization wave-function correction)

Formal expressions for the diagrams presented in Fig. 1 can be obtained both employing Sucher's symmetrized form [33] of the Gell-Mann–Low level shift [34], presented in some detail in [30] and [32] for the problem under consideration, and also by the two-time Green function method [35] which was applied to the radiative corrections to a magnetic interaction in [36] and [37]. The resulting energy shifts from the different diagrams due to a magnetic perturbing potential $\boldsymbol{A}$ are given by (in Feynman gauge, $\hbar = c = m_e = 1$, $e^2 = 4\pi\alpha$)

$$\Delta E_{\mathrm{SE,\,ve}} = e^2 \frac{\mathrm{i}}{2\pi} \int \mathrm{d}\,\boldsymbol{x} \int \mathrm{d}\,\boldsymbol{y} \int \mathrm{d}\,\boldsymbol{z} \int \mathrm{d}\omega\, \overline{a}_n(\boldsymbol{y})\, \gamma^\mu\, D_{F\,\mu\nu}(\boldsymbol{y},\boldsymbol{x},\omega) \times S_F(\boldsymbol{y},\boldsymbol{z},E_n-\omega)\, e\,\boldsymbol{\gamma}\cdot\boldsymbol{A}(\boldsymbol{z})\, S_F(\boldsymbol{z},\boldsymbol{x},E_n-\omega)\,\gamma^\nu\, a_n(\boldsymbol{x})\ , \quad (9)$$

$$\Delta E_{\mathrm{SE,\,wf,\,irred.}} = 2\,e^2 \frac{\mathrm{i}}{2\pi} \int \mathrm{d}\,\boldsymbol{x} \int \mathrm{d}\,\boldsymbol{y} \int \mathrm{d}\,\boldsymbol{z} \int \mathrm{d}\omega\, \overline{a}_n(\boldsymbol{y})\, \gamma^\mu\, D_{F\,\mu\nu}(\boldsymbol{y},\boldsymbol{x},\omega) \times S_F(\boldsymbol{y},\boldsymbol{x},E_n-\omega)\,\gamma^\nu \sum_{\substack{q\\ E_q\neq E_n}} \frac{\Phi_q(\boldsymbol{x})\Phi_q^\dagger(\boldsymbol{z})\,\gamma^0}{E_n-E_q}\, e\,\boldsymbol{\gamma}\cdot\boldsymbol{A}(\boldsymbol{z})\, a_n(\boldsymbol{z})$$

$$= 2 \sum_{\substack{q \\ E_q \neq E_n}} \frac{\langle a_n|\gamma^0 \Sigma(E_n)|\Phi_q\rangle\langle\Phi_q|e\,\boldsymbol{\alpha}\cdot\boldsymbol{A}|a_n\rangle}{E_n - E_q} \,, \tag{10}$$

where the self energy operator $\Sigma(E_n)$ was introduced,

$$\langle a|\gamma^0\Sigma(E)|b\rangle = e^2\,\frac{\mathrm{i}}{2\pi}\int \mathrm{d}\,\boldsymbol{x}\int \mathrm{d}\,\boldsymbol{y}\int \mathrm{d}\omega\,\overline{a}(\boldsymbol{y})\gamma^\mu\,D_{F\,\mu\nu}(\boldsymbol{y},\boldsymbol{x},\omega) \times S_F(\boldsymbol{y},\boldsymbol{x},E-\omega)\,\gamma^\nu\,b(\boldsymbol{x}) \,. \tag{11}$$

In (10), an additional factor 2 accounts for the two symmetrical diagrams Fig. 1, (c) and (e). In these equations, $S_F(\boldsymbol{x},\boldsymbol{y};E)\gamma_0$ denotes the time-independent Green function of a bound electron related to the four-dimensional electron propagator by

$$S_F(\mathrm{x},\mathrm{y}) = \frac{\mathrm{i}}{2\pi}\int \mathrm{d}E\,\mathrm{e}^{-\mathrm{i}(t_x-t_y)E}\sum_m \frac{\Phi_m(\boldsymbol{x})\overline{\Phi}_m(\boldsymbol{y})}{E-E_m(1-\mathrm{i}\eta)}$$
$$= \frac{\mathrm{i}}{2\pi}\int \mathrm{d}E\,\mathrm{e}^{-\mathrm{i}(t_x-t_y)E}\,S_F(\boldsymbol{x},\boldsymbol{y};E) \,. \tag{12}$$

It obeys the equation

$$\left[E - \left(\boldsymbol{\alpha}\cdot\boldsymbol{p} + \beta m + V_{\mathrm{nuc}}^{\mathrm{bind}}(\boldsymbol{x})\right)\right] S_F(\boldsymbol{x},\boldsymbol{y};E)\gamma_0 = \delta^3(\boldsymbol{x}-\boldsymbol{y}) \tag{13}$$

where $V_{\mathrm{nuc}}^{\mathrm{bind}}(\boldsymbol{x})$ is the nuclear binding potential. By Roman-style symbols we denote four-vectors, i.e, $\mathrm{x} = (t_x, \boldsymbol{x})$. The sums in (10) and (12) indicate summation and integration over the complete Dirac spectrum. Intermediate eigenstates to the Dirac equation with the binding potential included are denoted by Φ, intermediate eigenstates to the free Dirac equation by φ. In Feynman gauge the photon propagator $D_{F\,\mu\nu}(\mathrm{x},\mathrm{y})$ is given by

$$D_{F\,\mu\nu}(\mathrm{x},\mathrm{y}) = -g_{\mu\nu}\,\frac{1}{(2\pi)^4}\int \mathrm{d}\boldsymbol{k}\int \mathrm{d}\omega\,\frac{\mathrm{e}^{-\mathrm{i}\omega(t_x-t_y)}\,\mathrm{e}^{\mathrm{i}\boldsymbol{k}(\boldsymbol{x}-\boldsymbol{y})}}{\omega^2-\boldsymbol{k}^2+\mathrm{i}\eta} \tag{14}$$
$$= \int \frac{\mathrm{d}\omega}{2\pi}\,\mathrm{e}^{-\mathrm{i}\omega(t_x-t_y)}\,D_{F\,\mu\nu}(\boldsymbol{x},\boldsymbol{y},\omega) \,. \tag{15}$$

The reducible part of $\Delta E_{\mathrm{SE,wf}}$, i.e., the part of the diagram Fig. 1, (c) and (e), with the external state present in the propagator between the self-energy loop and the magnetic interaction, is given by [30,32]

$$\Delta E_{\mathrm{SE,\,wf,\,red.}} = \langle a_n|\,\gamma^0\,\frac{\partial}{\partial E}\Sigma(E)\Big|_{E=E_n}|a_n\rangle\langle a_n|e\,\boldsymbol{\alpha}\cdot\boldsymbol{A}|a_n\rangle \,. \tag{16}$$

The vacuum polarization contributions are given by

$$\Delta E_{\mathrm{VP,\,pot}} = -e^2\,\frac{\mathrm{i}}{2\pi}\int \mathrm{d}\boldsymbol{x}\int \mathrm{d}\boldsymbol{y}\int \mathrm{d}\boldsymbol{z}\,D_{F\,\mu\nu}(\boldsymbol{x},\boldsymbol{y},\omega=0)\int_{-\infty}^{\infty}\mathrm{d}E$$
$$\times\overline{a}_n(\boldsymbol{x})\gamma^\mu a_n(\boldsymbol{x})\,\mathrm{Tr}\left[\gamma^\nu S_F(\boldsymbol{y},\boldsymbol{z};E)\,e\,\boldsymbol{\gamma}\cdot\boldsymbol{A}(\boldsymbol{z})\,S_F(\boldsymbol{z},\boldsymbol{y};E)\right] \,, \tag{17}$$

$$\Delta E_{\mathrm{VP,\,wf,\,irred.}} = 2 \sum_{\substack{q \\ E_q \neq E_n}} \frac{\langle a_n | U_{\mathrm{VP}} | \Phi_q \rangle \langle \Phi_q | e\, \boldsymbol{\alpha} \cdot \boldsymbol{A} | a_n \rangle}{E_n - E_q} \,. \tag{18}$$

Again, the symmetry of two equally contributing diagrams was taken into account by an additional factor 2 in (18). A "reducible" part of the vacuum polarization contributions can be shown to vanish [32]. The vacuum polarization potential introduced in (18) is given by

$$\begin{aligned} U_{\mathrm{VP}}(\boldsymbol{x}) = &- e^2 \frac{\mathrm{i}}{2\pi} \int \mathrm{d}\boldsymbol{y}\, D_{F\,00}(\boldsymbol{x}, \boldsymbol{y}, \omega = 0) \\ &\times \int \mathrm{d}E\, \mathrm{Tr} \left[\sum_r \frac{\Phi_r(\boldsymbol{y}) \Phi_r^\dagger(\boldsymbol{y})}{E - E_r(1 - \mathrm{i}\eta)} \right] \,. \end{aligned} \tag{19}$$

A detailed derivation of the vacuum polarization potential is given by [38,39] (and references therein).

All expressions presented so far describe the energy shift due to a perturbing magnetic potential $\boldsymbol{A}$. The contribution to the g_J factor is easily derived from these expressions by applying (4). However, all derived expressions are only formal and require normalization. For the vacuum polarization expressions this procedure follows the standard scheme by decomposing the vacuum polarization potential into the (leading) Uehling part which is renormalized separately and the remaining finite Wichmann-Kroll part. For the wave-function correction the problem thus reduces to a proper calculation of the Uehling and Wichmann-Kroll parts of the vacuum polarization potentials according to the procedures given in [38,39]. For the case of carbon, we obtain contributions to the g factor of $-8.55285(1) \times 10^{-9}$ from the Uehling part of the vacuum polarization potential and $3.28(1) \times 10^{-12}$ from the Wichmann-Kroll part. The numerical uncertainties are by far less than any other error discussed in this article.

For the potential correction, no Uehling-like contribution exists for a homogeneous external magnetic field [31,32], and the remaining Wichmann-Kroll part can be written as [40]

$$\begin{aligned} \Delta E^{\mathrm{WK}}_{\mathrm{VP,\,pot}} = &- \frac{e^2}{\pi^2} \sum_{\kappa = \pm 1}^{\infty} \sum_{\kappa' = \tilde{\kappa}_{-1}}^{\tilde{\kappa}_1} \\ &\times \sum_{l=0}^{\infty} (2l+1) \int_0^\infty \mathrm{d}k \langle a_n | \alpha^\mu j_l(k\,x) \mathbf{C}^l(\hat{\boldsymbol{x}}) | a_n \rangle \\ &\times \left\{ \sum_{\substack{q \\ E_q > 0}} \sum_{\substack{r \\ E_r < 0}} \frac{\langle \Phi_{q,\kappa} | \alpha_\mu\, j_l(k\,y)\, \mathbf{C}^l(\hat{\boldsymbol{y}})) | \Phi_{r,\kappa'} \rangle \langle \Phi_{r,\kappa'} | e\, \boldsymbol{\alpha} \cdot \boldsymbol{A} | \Phi_{q,\kappa} \rangle}{E_{q,\kappa} - E_{r,\kappa'}} \right. \\ &\left. - \sum_{\substack{s \\ E_s > 0}} \sum_{\substack{t \\ E_t < 0}} \frac{\langle \varphi_{s,\kappa} | \alpha_\mu\, j_l(k\,y)\, \mathbf{C}^l(\hat{\boldsymbol{y}}) | \varphi_{t,\kappa'} \rangle \langle \varphi_{t,\kappa'} | e\, \boldsymbol{\alpha} \cdot \boldsymbol{A} | \varphi_{s,\kappa} \rangle}{E_s - E_t} \right\} \,. \end{aligned} \tag{20}$$

Here, $\tilde{\kappa}_{-1} = -\kappa - 1$, $\tilde{\kappa}_0 = \kappa$, $\tilde{\kappa}_1 = -\kappa + 1$, where κ indicates the Dirac angular momentum quantum number (cf., e.g., [41]). Spherical Bessel functions are denoted by j_l and $\mathbf{C}^l(\hat{\boldsymbol{x}})$ is a spherical tensor operator (e.g. [42]), depending on $\hat{\boldsymbol{x}} = \boldsymbol{x}/|\boldsymbol{x}|$ and defined by

$$C_m^l(\hat{\boldsymbol{x}}) = \sqrt{\frac{4\pi}{(2l+1)}} Y_l^m(\hat{\boldsymbol{x}}) \ . \tag{21}$$

$Y_m^l(\hat{\boldsymbol{x}})$ denotes a spherical harmonic. The scalar product between two tensor operators $\mathbf{C}^l(\hat{\boldsymbol{y}}) \cdot \mathbf{C}^l(\hat{\boldsymbol{x}})$ is given by

$$\mathbf{C}^l(\hat{\boldsymbol{y}}) \cdot \mathbf{C}^l(\hat{\boldsymbol{x}}) = \sum_{m=-l}^{l} (-1)^m C_m^l(\hat{\boldsymbol{y}})\, C_{-m}^l(\hat{\boldsymbol{x}}) \ . \tag{22}$$

This scalar product is implicitly assumed in all formulas with $\mathbf{C}^l$ present in two matrix elements.

The sums over intermediate bound and free states are carried out by generating a complete set of intermediate states utilizing the space-discretization method of Salomonson and Öster [43]. The functions obtained by this method are given on a few finite sets of grid points only. The integrations are also carried out on the same grids, if the grid sizes prove to be sufficient for an accurate calculation which is controlled by extrapolating the number of grid points to infinity. For high k, the spherical Bessel functions are strongly oscillating, and therefore the grid-valued functions have to be interpolated to continuous space using Lagrange polynomials [44] to obtain the proper values of the matrix elements. For details of the method, we refer to [43]. The outer k integration is handled numerically, using Gauss-Legendre and Gauss-Laguerre quadrature formulas. Finally, the sum over κ is carried out by evaluating a finite number of summands and performing a polynomial expansion to infinity. For the correction under consideration here, the summands up to $|\kappa| \leqslant 30$ can be evaluated without problems for higher Z. For $Z \leqslant 20$, however, the convergence becomes very poor. Higher $|\kappa|$ are prevented by the numerical accuracy of our present code, and for $Z \leqslant 10$ almost no meaningful value is obtained at all. However, contrary to the vertex contribution mentioned above, the total $\Delta E_{\mathrm{VP,\,pot}}$ contribution is rather small for low Z and thus the total precision of our calculations is hardly influenced by this drawback. We consider the contribution for $^{12}C^{5+}$ to be much less than 1×10^{-10} but with an error of 3×10^{-10} [32].

Our way to deal with the divergences of the self-energy expressions is to evaluate the bound-state electron propagators into powers of the nuclear binding potential and to isolate the mass and charge divergences which are only present in the lowest order terms. These terms are treated analytically in momentum space, and after cancelling the divergences between different diagrams a finite result is obtained. The finite higher-order terms are evaluated in coordinate space by employing the full yet unrenormalized expression and subtracting the divergent lower-order parts in the calculation. The procedure outlined so far coincides with

that employed by Snyderman [45] and has been described in detail in [46] for the QED corrections to the hyperfine structure splitting.

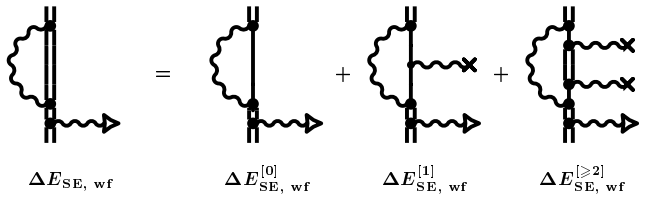

Fig. 2. The decomposition of $\Delta E_{\mathrm{SE,\,wf,\,irred.}}$ into terms appropriate for removing divergences and for numerical calculation. A photon line terminated by a cross denotes one interaction with the nuclear binding potential. The labels under the diagrams correspond to the terminology used in the text. The superscript in brackets indicates the number of interactions with the nuclear binding potential. For brevity the index "irred." was omitted on all labels

The decomposition of the irreducible part of the self-energy wave-function correction term is depicted in Fig. 2. The divergent terms are these with zero and one interaction in the binding potential present, below referred to as "zero-potential term" and "one-potential term", respectively. The charge divergences cancel between both terms. In addition, a mass counter term δm has to be subtracted to obtain proper mass renormalization similar to the case of the free self energy [47] (for our schemes see also [44]). The zero- and one-potential terms are then semianalytically evaluated in momentum space (for details cf. [32]) whereas the remaining part $\Delta E^{[\geqslant 2]}_{\mathrm{SE,\,wf,\,irred.}}$ is calculated in coordinate space. After some algebra it can be written as

$$
\begin{aligned}
\Delta E^{[\geqslant 2]}_{\mathrm{SE,\,wf,\,irred.}} = -\frac{e^2}{2\pi^2}\sum_{l=0}^{\infty}(2l+1)\int \mathrm{d}k\,k \\
\times\Bigg\{\sum_p \frac{\langle a_n|\alpha^\mu j_l(k\,y)\mathbf{C}^l(\hat{\boldsymbol{y}})|\Phi_p\rangle\langle\Phi_p|j_l(k\,x)\mathbf{C}^l(\hat{\boldsymbol{x}})\alpha_\mu|\delta a_n\rangle}{E_n-E_p-\mathrm{sign}(E_p)k} \\
-\sum_r \frac{\langle a_n|\alpha^\mu j_l(k\,y)\mathbf{C}^l(\hat{\boldsymbol{y}})|\varphi_r\rangle\langle\varphi_r|j_l(k\,x)\mathbf{C}^l(\hat{\boldsymbol{x}})\alpha_\mu|\delta a_n\rangle}{E_n-E_r-\mathrm{sign}(E_r)k} \\
-\sum_{s,r}\Bigg[\frac{\langle a_n|\alpha^\mu j_l(k\,y)\mathbf{C}^l(\hat{\boldsymbol{y}})|\varphi_s\rangle\langle\varphi_s|V^{\mathrm{bind}}_{\mathrm{nuc}}|\varphi_r\rangle}{[E_n-E_s-\mathrm{sign}(E_s)k]} \\
\times\frac{\langle\varphi_r|j_l(k\,x)\mathbf{C}^l(\hat{\boldsymbol{x}})\alpha_\mu|\delta a_n\rangle}{[E_n-E_r-\mathrm{sign}(E_r)k]}\,F(s,r)\Bigg]\Bigg\}\,. \qquad (23)
\end{aligned}
$$

The function F is introduced here to denote part of the energy denominator,

$$F(s,r) = 1 + [\mathrm{sign}(E_r) - \mathrm{sign}(E_s)]\ \frac{k}{E_r - E_s} \tag{24}$$

and

$$|\delta a_n\rangle = \sum_{\substack{q \\ E_q \neq E_n}} \frac{|\Phi_q\rangle\langle\Phi_q|e\,\boldsymbol{\alpha}\cdot\boldsymbol{A}|a_n\rangle}{E_n - E_q}\ . \tag{25}$$

If E_n represents the lowest positive energy eigenvalue of the bound Dirac spectrum, the further evaluation of (23) is straightforward employing standard methods. In the present work this is the case as we consider only the $1S_{1/2}$ state. The numerical evaluation scheme is similar to that described already. After including the results for $\Delta E^{[0]}_{\mathrm{SE,\,wf,\,irred.}}$ and $\Delta E^{[1]}_{\mathrm{SE,\,wf,\,irred.}}$, we obtain a total contribution of $g_{\mathrm{SE,\,wf,\,irred.}} = 3.40647(4)\times 10^{-5}$ for the irreducible wave function contribution in the case of $^{12}C^{5+}$. The error is mainly due to extrapolating the number of partial waves l to infinity and might be reduced by employing other summation schemes, e.g., the convergence acceleration methods presented by Jentschura *et al.*([49] and references therein).

The reducible part of the self-energy wave-function correction, Eq. (16), also contains an ultraviolet divergent part which is cancelled by a similar expression present in the vertex correction term, Eq. (9). In addition, an infrared divergence exists which mutually cancels as well. These two terms are therefore evaluated together. Both contributions are decomposed into a zero-potential term with the full electron propagators within the loop replaced by free ones, and the remaining "many"-potential part, similar to the irreducible wave-function contribution. Again, we refer to [32] for the lengthy zero-potential parts and only the results the many-potential parts are shown here,

$$\begin{aligned}\Delta E^{[\geqslant 1]}_{\mathrm{SE,\,wf,\,red.}} = \langle a_n|e\,\boldsymbol{\alpha}\cdot\boldsymbol{A}|a_n\rangle \times \frac{e^2}{4\pi^2}\sum_{l=0}^{\infty}(2l+1)\int \mathrm{d}k\,k \\ \times\left\{\sum_p \frac{\langle a_n|\alpha^\mu j_l(k\,y)\mathbf{C}^l(\hat{\boldsymbol{y}})|\Phi_p\rangle\langle\Phi_p|j_l(k\,x)\mathbf{C}^l(\hat{\boldsymbol{x}})\alpha_\mu|a_n\rangle}{\left[E_n - E_p - \mathrm{sign}(E_p)k\right]^2}\right. \\ \left. -\sum_r \frac{\langle a_n|\alpha^\mu j_l(k\,y)\mathbf{C}^l(\hat{\boldsymbol{y}})|\varphi_r\rangle\langle\varphi_r|j_l(k\,x)\mathbf{C}^l(\hat{\boldsymbol{x}})\alpha_\mu|a_n\rangle}{\left[E_n - E_r - \mathrm{sign}(E_r)k\right]^2}\right\}\ .\end{aligned} \tag{26}$$

The first term is infrared divergent for $l = 0$ and $\mu = 0$, if the energy of the intermediate state p coincides with E_n. A similar term with opposite sign occurs from the vertex term which will be presented next. Therefore the sum of both terms is infrared finite. In performing their numerical evaluation, we explicitly exclude the terms with $l = 0$, $\mu = 0$ from the calculation. The vertex part is given by

$$\Delta E^{[\geqslant 1]}_{\mathrm{SE,\,ve}} = -\frac{e^2}{4\pi^2}\sum_{l=0}^{\infty}(2l+1)\int \mathrm{d}k\,k$$

$$\times \Bigg\{ \sum_{q,r} \Bigg[\frac{\langle a_n|\, a^\mu\, j_l(k\,y)\, \mathbf{C}^l(\hat{\boldsymbol{y}})|\Phi_q\rangle\langle\Phi_q|\, e\,\boldsymbol{\alpha}\cdot\boldsymbol{A}\,|\Phi_r\rangle}{[E_n - E_q - \mathrm{sign}(E_q)\,k]} \times \frac{\langle\Phi_r|\, a_\mu\, j_l(k\,x)\, \mathbf{C}^l(\hat{\boldsymbol{x}})|a_n\rangle}{[E_n - E_r - \mathrm{sign}(E_r)\,k]} F(q,r) \Bigg] - \sum_{p,s} \Bigg[\frac{\langle a_n|\, a^\mu\, j_l(k\,y)\, \mathbf{C}^l(\hat{\boldsymbol{y}})|\varphi_p\rangle\langle\varphi_p|\, e\,\boldsymbol{\alpha}\cdot\boldsymbol{A}\,|\varphi_s\rangle}{[E_n - E_p - \mathrm{sign}(E_p)\,k]} \times \frac{\langle\varphi_s|\, a_\mu\, j_l(k\,x)\, \mathbf{C}^l(\hat{\boldsymbol{x}})|a_n\rangle}{[E_n - E_s - \mathrm{sign}(E_s)\,k]} F(p,s) \Bigg] \Bigg\} \,. \tag{27}$$

The numerical evaluation of this vertex expression proved to be difficult in particular for low Z. To overcome this, the terms containing one interaction with the external nuclear binding potential were also separated and calculated in a semianalytical way. A detailed discussion of the problem and the procedure to solve it is given in [27], numerical details can also be found in [40]. For $^{12}C^{5+}$, we end up with a total contribution of $g_{\mathrm{SE,\,wf,\,red.}} + g_{\mathrm{SE,\,ve.}} = 2.289\,607\,7(5) \times 10^{-3}$ where the error again represents the numerical uncertainty. This contribution contains also the g factor of the free electron and is therefore by far the largest from all diagrams in Fig. 1.

4 QED Effects of Higher Orders

The diagrams of order $(\alpha/\pi)^2$, are depicted in Fig. 3. These and diagrams of even higher order have not yet been evaluated non-perturbatively in $(Z\alpha)$. Leading terms of a $(Z\alpha)$ expansion can be derived from [48] to be

$$g_{J,\,(\alpha/\pi)^2(Z\alpha)^2} = 2\,A_1^{(4)} \left(\frac{\alpha}{\pi}\right)^2 \frac{(Z\alpha)^2}{6} \tag{28}$$

where $A_1^{(4)}$ is the coefficient of $(\alpha/\pi)^2$ in the (α/π) expansion of $g_S/2$ ([11] and references therein) which is given by $A_1^{(4)} = 197/144 + (1/2 - 3\ln 2)\,\zeta(2) + 3/4\,\zeta(3) = -0.328\,478\,965\ldots$. Equation (28) yields $g_{J,\,(\alpha/\pi)^2(Z\alpha)^2} = -1.1 \times 10^{-9}$ for $^{12}C^{5+}$. This is a result of the leading terms of a $(Z\alpha)$ expansion, however. For the Lamb shift, where second order effects were investigated closer, it is known that $Z\alpha$ expansions tend to fail even for low to medium Z [1] and non-perturbative methods in $(Z\alpha)$ can cope with the expansions even for hydrogen [49]. Therefore the result (28) should be considered with care and its uncertainty should be taken at least as the size of its value.

Recently, Karshenboim [50] has presented evaluations of a few diagrams of Fig. 3 which go beyond the $(Z\alpha)^2$ terms. As long as not all diagrams of Fig. 3 are included in such an evaluation, it is meaningless, however, to include any numerical value into our present estimate. For details, we refer to [50].

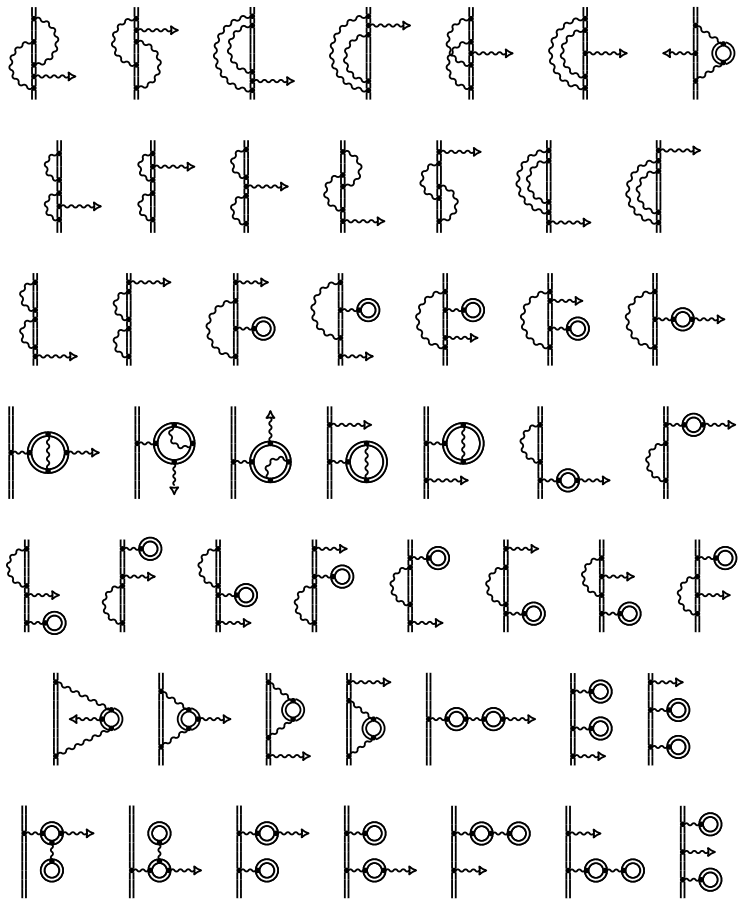

Fig. 3. QED diagrams of order $(\alpha/\pi)^2$ contributing to g_J

5 Total Theoretical Value

In Table 1, we present a listing of all theoretical contributions to $g_{J,\,1S_{1/2}}(^{12}C^{5+})$ known so far. All values were obtained employing $1/\alpha = 137.035\,989\,5$ in the calculations. The recommended value which was published recently [51], $1/\alpha = 137.035\,999\,76$, does not affect the total result by more than 1×10^{-10}. The bound-state QED value of order (α/π) was obtained by subtracting the contributions of this order to g_S from the total value. It should be compared with the result of the leading terms of the $(Z\alpha)$ expansion [12] which is also given in the table. The difference is about 1×10^{-7}. This is clearly visible at an experimental precision of a few times 10^{-9}. It can therefore be expected that with increasing Z or increasing experimental precision any $(Z\alpha)$ expansion might not be sufficient

also for order $(\alpha/\pi)^2$ and the next tasks of theory should be the evaluation of the diagrams shown in Fig. 3 and a full calculation of the recoil effect without any expansion in $(Z\alpha)$. The first of these tasks might prove to be particularly difficult as even the ten diagrams of order α^2 for the Lamb shift (on which the 50 diagrams of Fig. 3 are based) are not yet completely evaluated ([1,52,53,54,55], and references therein).

Table 1. Known theoretical contributions to the g_J factor of an electron bound in the ground state of $^{12}C^{5+}$. All values are given in units of 10^{-9}. The error estimates are discussed in the text. If no error is given, it is less than 0.5×10^{-10}. The errors for the "total" value are due to the $(Z\alpha)$ expansion for the recoil contribution, the numerical uncertainties for the QED effects of order (α/π), and the estimated error for the bound-state QED contribution of order $(\alpha/\pi)^2$. In order not to underestimate any systematic effect, the numerical errors were linearly added

Contribution to g_J	numerical value (in 10^{-9})
Breit	1 998 721 354.2
fin. nuc. size	0.4
recoil	87.5(9)
VP, wf.	−8.5
VP, pot.	0.0(3)
SE, wf, irred.	34 064.7(4)
SE, ve + SE, wf, red.	2 289 607.7(5)
free QED, $(\alpha/\pi)^2$ to $(\alpha/\pi)^4$	−3 515.1
bound QED, $(\alpha/\pi)^2\,(Z\alpha)^2$	−1.1(11)
total:	2 001 041 589.8(9)(12)(11)
total QED, order (α/π):	2 323 663.9(12)
free QED, order (α/π):	2 322 819.6
bound QED, order (α/π):	844.3(12)
(in $(Z\alpha)$ exp., $(Z\alpha)^2$ term:	742.2)

To compare our theoretical result with the current experimental data, we refer to the overview article [25] given elsewhere in this book. The results are in reasonable agreement and thus the g_J factor experiment on hydrogenlike carbon in combination with our theoretical results forms one of the most stringent QED tests for systems with $Z > 1$.

6 Acknowledgements

T. B. wants to thank the organizers for inviting him to the conference. We acknowledge a continuous fruitful collaboration with the experimental team of the g factor measurements, H. Häffner, N. Hermanspahn, H.-J. Kluge, W. Quint, S. Stahl, J. Verdú, and G. Werth. We are also grateful to A.-M. Mårtensson-Pendrill, S. G. Karshenboim, K. Pachucki, V. M. Shabaev, G. Soff, and V. A.

Yerokhin for many valuable discussions on the subject, and to E. E. B. Campbell for the extremely stimulating atmosphere within the Göteborg Atomic and Molecular Physics group where most of the work was performed. Financial support was obtained by the European Union under the contract number ERB FMRX CT 97-0144 within the EUROTRAPS network.

References

1. P. J. Mohr, G. Plunien, and G. Soff: Physics Reports **293**, 227 (1998)
2. H. F. Beyer, G. Menzel, D. Liesen, A. Gallus, F. Bosch, R. Deslattes, P. Indelicato, T. Stöhlker, O. Klepper, R. Moshammer, F. Nolden, H. Eickhoff, B. Franzke, and M. Steck: Z. Phys. D **35**, 169 (1995)
3. H. F. Beyer and T. Stöhlker: 'Test of QED in high-Z hydrogen-like systems'. In: *Frontier tests of QED and Physics of the Vacuum*, ed. by E. Zavattini, D. Bakalov, and C. Rizzo (Heron Press, Sofia 1994) pp. 356–270
4. J. Schweppe, A. Belkacem, L. Blumenfeld, N. Claytor, B. Feinberg, H. Gould, V. E. Kostroun, L. Levy, S. Misawa, J. R. Mowat, and M. H. Prior: Phys. Rev. Lett. **66**, 1434 (1991)
5. P. Beiersdorfer, A. Osterheld, S. R. Elliott, M. H. Chen, D. Knapp, and K. Reed: Phys. Rev. A **52**, 2693 (1995)
6. P. Beiersdorfer, A. L. Osterheld, J. H. Scofield, J. R. Crespo López-Urrutia, and K. Widmann: Phys. Rev. Lett. **80**, 3022 (1998)
7. I. Klaft, S. Borneis, T. Engel, B. Fricke, R. Grieser, G. Huber, T. Kühl, D. Marx, R. Neumann, S. Schröder, P. Seelig, and L. Völker: Phys. Rev. Lett. **73**, 2425 (1994)
8. J. R. Crespo López-Urrutia, P. Beiersdorfer, D. W. Savin, and K. Widmann: Phys. Rev. Lett. **77**, 826 (1996)
9. J. R. Crespo López-Urrutia, P. Beiersdorfer, K. Widmann, B. B. Birkett, A.-M. Mårtensson-Pendrill, and M. G. H. Gustavsson: Phys. Rev. A **57**, 879 (1998)
10. R. S. Van Dyck, Jr., P. B. Schwinberg, and H. G. Dehmelt: Phys. Rev. Lett. **59**, 26 (1987)
11. V. W. Hughes and T. Kinoshita: Rev. Mod. Phys. **71**, 133 (1999)
12. H. Grotch: Phys. Rev. Lett. **24**, 39 (1970)
13. H. Grotch: Phys. Rev. A **2**, 1605 (1970)
14. H. Grotch and R. A. Hegstrom: Phys. Rev. A **4**, 59 (1971)
15. R. Faustov: Nuovo Cimento **69A**, 37 (1970)
16. R. Faustov: Phys. Lett. **33B**, 422 (1970)
17. F. E. Close and H. Osborn: Phys. Lett. **34B**, 400 (1971)
18. L. C. Balling and F. M. Pipkin: Phys. Rev. **139**, A19 (1965)
19. F. G. Walther, W. D. Phillips, and D. Kleppner: Phys. Rev. Lett. **28**, 1159 (1972)
20. J. S. Tiedeman and H. G. Robinson: Phys. Rev. Lett. **39**, 602 (1977)
21. C. E. Johnson and H. G. Robinson: Phys. Rev. Lett. **45**, 250 (1980)
22. K. Hermanspahn, W. Quint, S. Stahl, M. Tönges, G. Bollen, H.-J. Kluge, R. Ley, R. Mann, and G. Werth: Acta Phys. Pol. **B 27**, 357 (1996)
23. M. Diederich, H. Häffner, N. Hermanspahn, M. Immel, H. J. Kluge, R. Ley, R. Mann, S. Stahl, W. Quint, J. Verdú, and G. Werth: 'The g-faktor of hydrogen-like ions'. In: *Trapped charged particles and fundamental physics, AIP conference proceedings 457*, ed. by D. H. E. Dubin and D. Schneider (American Institute of Physics, Woodbury, New York 1999) pp. 43–51

24. N. Hermanspahn, H. Häffner, H.-J. Kluge, W. Quint, S. Stahl, J. Verdú, and G. Werth: Phys. Rev. Lett. **84**, 427 (2000)
25. G. Werth, H. Häffner, N. Hermanspahn, H.-J. Kluge, W. Quint, S. Stahl, and J. Verdú: *this edition*, pp. 204–220
26. G. Breit: Nature (London) **122**, 649 (1928)
27. T. Beier, I. Lindgren, H. Persson, S. Salomonson, and P. Sunnergren: Hyperfine Interactions **127**, 339 (2000)
28. J. Schwinger: Phys. Rev. **73**, 416 (1948)
29. J. Schwinger Phys. Rev. **76**, 790 (1949)
30. S. A. Blundell, K. T. Cheng, and J. Sapirstein: Phys. Rev. A **55**, 1857 (1997)
31. H. Persson, S. Salomonson, P. Sunnergren, and I. Lindgren: Phys. Rev. A **56**, R2499 (1997)
32. T. Beier, I. Lindgren, H. Persson, S. Salomonson, P. Sunnergren, H. Häffner, and N. Hermanspahn: Phys. Rev. A **62**, 032510
33. J. Sucher: Phys. Rev. **107**, 1448 (1957)
34. M. Gell-Mann and F. Low: Phys. Rev. **84**, 350 (1951)
35. V. M. Shabaev and I. G. Fokeeva: Phys. Rev. A **49**, 4489 (1994)
36. M. B. Shabaeva and V. M. Shabaev: Phys. Rev. A **52**, 2811 (1995)
37. T. Beier: Physics Reports, to be published
38. G. Soff and P. Mohr: Phys. Rev. A **38**, 5066 (1988)
39. H. Persson, I. Lindgren, S. Salomonson, and P. Sunnergren: Phys. Rev. A **48**, 2772 (1993)
40. P. Sunnergren: Complete One-Loop QED Calculations for Few-Electron Ions Ph.D. dissertation, Göteborgs universitet och Chalmers tekniska högskola, Göteborg (1998)
41. M. E. Rose: *Relativistic Electron Theory*. (John Wiley & Sons, New York 1961)
42. I. Lindgren and J. Morrison: *Atomic Many-Body Theory*, 2nd edition. (Springer, Berlin 1986)
43. S. Salomonson and P. Öster: Phys. Rev. A **40**, 5548 (1989)
44. H. Persson, I. Lindgren, and S. Salomonson: Physica Scripta **T46**, 125 (1993)
45. N. J. Snyderman: Ann. Phys. (New York) **211**, 43 (1991)
46. P. Sunnergren, H. Persson, S. Salomonson, S. M. Schneider, I. Lindgren, and G. Soff: Phys. Rev. A **58**, 1055 (1998)
47. M. Baranger, H. A. Bethe, and R. P. Feynman: Phys. Rev. **92**, 482 (1953)
48. M. I. Eides and H. Grotch: Ann. Phys. (N.Y.) **260**, 191 (1997)
49. U. D. Jentschura, P. J. Mohr, and G. Soff: Phys. Rev. Lett. **82**, 53 (1999)
50. S. G. Karshenboim: Phys. Lett. **A 266**, 380 (2000); *this edition*, pp. 651–663
51. P. J. Mohr and B. N. Taylor: Rev. Mod. Phys. **72**, 351 (2000)
52. V. A. Yerokhin: Phys. Rev. A **62**, 012508 (2000)
53. V. A. Yerokhin: *this edition*, pp. 800–809
54. I. A. Goidenko, L. N. Labzowsky, A. V. Nefiodov, G. Plunien, and G. Soff: Phys. Rev. Lett. **83** 2312 (1999)
55. I. A. Goidenko, L. N. Labzowsky, A. V. Nefiodov, G. Plunien, S.Zschocke, and G. Soff: *this edition*, pp. 619–636